Spanning the full range of neutron star properties within a microscopic description

Presented in AAPCOS-2023, SINP

Tuhin Malik, Márcio Ferreira, Constança Providência

Universidade de Coimbra, Portugal

UNIVERSIDADE DE COIMBRA

The dense matter equation of state (EOS)

- A neutron star (NS), also known as a pulsar, is one of the densest and most compact objects in the universe.
- A significant probe to reduce uncertainty can be the NS maximum mass, radii, moments of inertia, and tidal Love numbers, which are all accessible to observation.
- The NS core composition remains a mystery

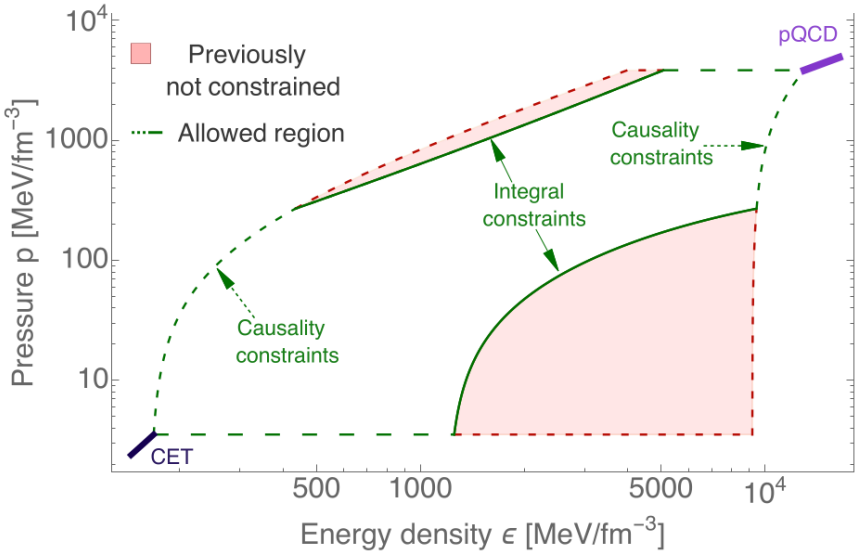

Phys. Rev. Lett. 128, 202701 (2022), 2111.05350

Probing the interior of Neutron Stars

- Neutrons stars provide a laboratory for testing
  - nuclear physics: high density, highly asymmetric matter
  - QCD: deconfinement, quark matter, superconducting phases
- mass-radius $\rightarrow$ equation of state $\rightarrow$ composition?

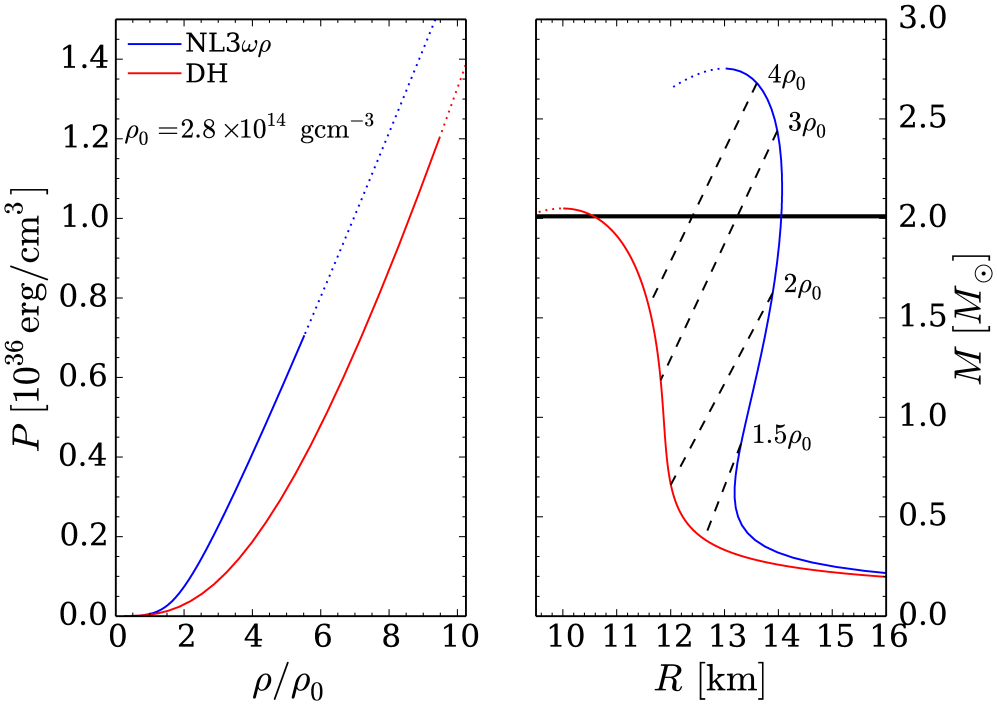

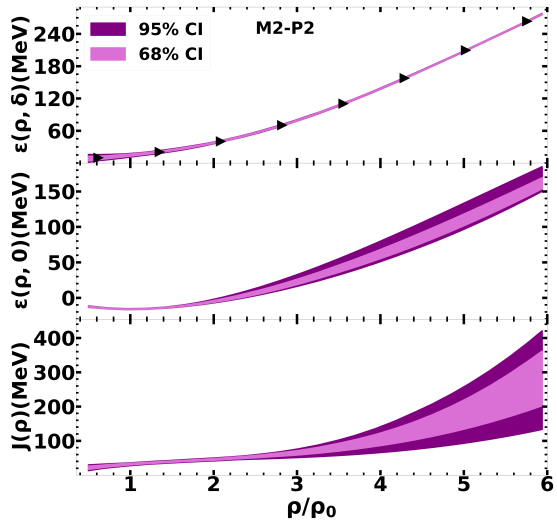

Sk Md Adil Imam et al PRC 105, 015806 (2022)
see also

- Tovar et al PRD 104 (2021)
- Mondal & Gulminelli PRD 105 (2022)
- Essick PRL 127 192701 (2021)

The possible scenario

- nucleon: Malik et al and B.K. Agrawal et al Astrophys.J. 930 (2022), Malik and B.K. Agrawal et al PRC Letter 106 (2022), Bikram Keshari Pradhan and Debarati Chatterjee et al Nucl.Phys.A 1030 (2023)
- hyperons: S. Weissenborn et al NPA 881 (2012), Micaela Oertel et al EPJA 52 (2016),Malik and Providência PRD 106 (2022)
- quark matter: Annala et al Nature Phys., 16, 907 (2020), Gorda et al arXiv:2212.10576 (2022)
- (anti) kaons: Banik et al. Phys.Rev.C 78 (2008), Char & Banik Phys. Rev. C 90(2014), Banik & Bandyopadhyay, Phys.Rev.C 64 (2001)
- dark matter
  - admixed: Arpan Das et al Phys.Rev.D 99 (2019), Violeta Sagun et al Phys.Rev.D 102 (2020)
  - two fluid: Arpan Das et al Phys.Rev.D 105 (2022), Violetta Sagun et al Phys.Rev.D 105 (2022)
- modified gravity: K. Nobleson et al JCAP 08 (2021)

Motivation

- Sounds speed describes how stiff matter is.
- The determination of the sound speed c_s^2 in NS is an important unresolved issue.
- At asymptotically high densities, the conformal symmetry of QCD is restored, and the sound speed approaches $c_s^2 = 1/3$, which is realized in ultrarelativistic fluids.
- Generally, in the microscopic model, c_s^2 tends to increase monotonically or saturates.

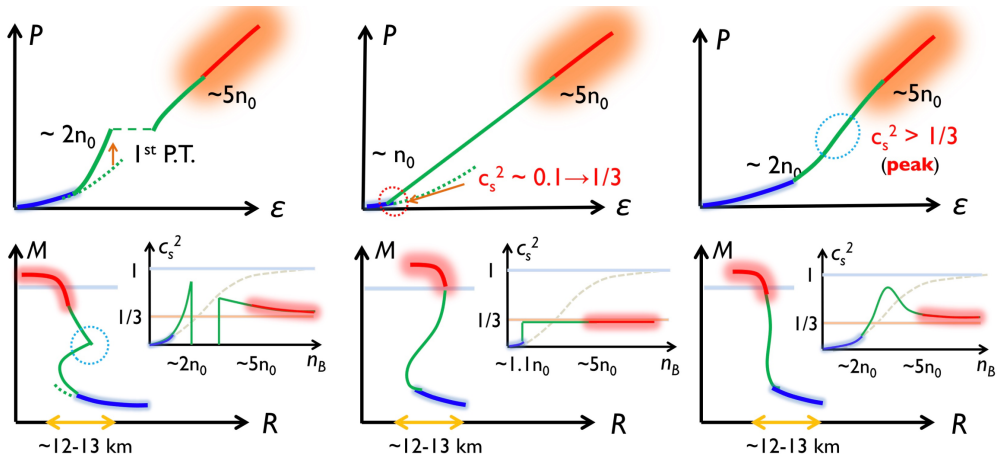

arxiv: 2011.10940

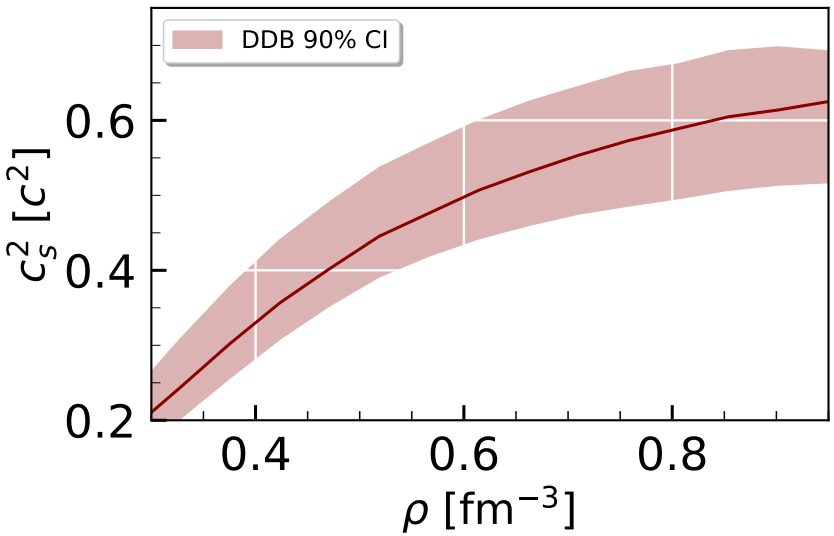

Malik et al Astrophys.J. 930 (2022) 1, 17

Motivation

- The agnostic approach:
  - L. Lindblom et al, Phys. Rev. D 86, 084003 (2012), arXiv:1207.3744.
  - A. Kurkela et al, Astrophys. J. 789, 127 (2014), arXiv:1402.6618.
  - E. R. Most et al, Phys. Rev. Lett. 120, 261103 (2018), arXiv:1803.00549.
  - E. Lope Oter et al, J. Phys. G 46, 084001 (2019), arXiv:1901.05271.
  - E. Annala et al, Nature Phys. 16, 907 (2020), arXiv:1903.09121., E. Annala et al, arXiv:2105.05132
  - Rahul Somasundaram et al, arXiv : 2112.08157
  - Sinan Altiparmak et al, arXiv: 2203.14974
- What do a minimal set of nuclear matter constraints together with a $2M_{\odot}$ condition tell us about the NS EOS based on a microscopic model?
- Can we extract nuclear matter properties from neutron star matter EOS?

Synopsis

To answer the motivation questions we:

- Will generate a set of EOS based on a microscopic model
- Include causality
- Restrict parameters imposing minimal constraints
- Access to nuclear saturation properties of different orders
- Analyze the speed of sound of generated EOS

RMF EOS from a Bayesian approach

EOS: relativistic mean field description

RMF Lagrangian for stellar matter

- Lagrangian density
  - Lorentz-covariant Lagrangian with baryon densities and meson fields
  - causal by construction

$$\mathcal{L} = \mathcal{L}_N + \mathcal{L}_M + \mathcal{L}_{NL},$$

- Baryonic contribution:

$$\mathcal{L}_N = \bar{\Psi}\left[\gamma^\mu \left(i\partial_\mu - g_\omega \omega_\mu - g_\varrho \boldsymbol{t}\cdot\boldsymbol{\varrho}_\mu\right) - \left(m - g_\sigma \phi\right)\right]\Psi,$$

- Meson contribution

$$\begin{aligned}\mathcal{L}_M =& \frac{1}{2}\left[\partial_\mu\phi\partial^\mu\phi - m_\sigma^2\phi^2\right] - \frac{1}{4}F^{(\omega)}_{\mu\nu}F^{(\omega)\mu\nu} + \frac{1}{2}m_\omega^2\omega_\mu\omega^\mu \\ & - \frac{1}{4}\boldsymbol{F}^{(\varrho)}_{\mu\nu}\cdot\boldsymbol{F}^{(\varrho)\mu\nu} + \frac{1}{2}m_\varrho^2\boldsymbol{\varrho}_\mu\cdot\boldsymbol{\varrho}^\mu.\end{aligned}$$

$$\begin{aligned}\mathcal{L}_{NL} =& -\frac{1}{3}bg_\sigma^3(\sigma)^3 - \frac{1}{4}cg_\sigma^4(\sigma)^4 + \frac{\xi}{4!}(g_\omega\omega_\mu\omega^\mu)^4 \\ & + \Lambda_\omega g_\varrho^2\boldsymbol{\varrho}_\mu\cdot\boldsymbol{\varrho}^\mu g_\omega^2\omega_\mu\omega^\mu\end{aligned}$$

Nuclear matter properties at saturation

- Taylor expansion, parabolic approximation

$$
\begin{aligned}
\frac{E_{\mathrm{nuc}}}{A}(n,\delta) &= \frac{E_{\mathrm{SNM}}}{A}(n) + S(n)\,\delta^2, \\
S(n) &= \frac{1}{2}\left.\frac{\partial^2 E_{\mathrm{nuc}}/A}{\partial \delta^2}\right|_{\delta=0}, \\
\frac{E_{\mathrm{SNM}}}{A}(n) &= E_0 + \frac{K_0}{2}\eta^2 + \frac{J_0}{3!}\eta^3 + \frac{Z_0}{4!}\eta^4, \\
S(n) &= E_{\mathrm{sym}} + L_{\mathrm{sym}}\eta + \frac{K_{\mathrm{sym}}}{2}\eta^2 + \frac{J_{\mathrm{sym}}}{3!}\eta^3 + \frac{Z_{\mathrm{sym}}}{4!}\eta^4,
\end{aligned}
$$

$$
\delta = (n_p - n_n)/n, \qquad \eta = (n - n_0)/(3n_0)
$$

Bayesian estimation of model parameters

Bayesian Inference:

$$P(\theta \mid D) = \frac{\mathcal{L}(D \mid \theta) P(\theta)}{\mathcal{Z}}$$

- The θ is the model parameter vector and D is the set of fit data.
- $P(\theta \mid D)$ is the joint posterior distribution of the parameters.
- $\mathcal{L}(D \mid \theta)$ is the likelihood function.
- $P(\theta)$ is the prior distribution for the model parameters.
- $\mathcal{Z}$ is the evidence. It can be obtained by complete marginalization of the likelihood function.

The marginalized posterior distribution for a parameter θ_i:

$$P(\theta_i \mid D) = \int P(\theta \mid D) \prod_{k \neq i} d\theta_k$$

Gaussian likelihood function

$$\mathcal{L}(D \mid \theta) = \prod_j \frac{1}{\sqrt{2\pi\sigma_j^2}} e^{-\frac{1}{2}\left(\frac{d_j - m_j(\theta)}{\sigma_j}\right)^2}$$

- The index j runs over all the data points.
- The d_j and m_j are the data and corresponding model values, respectively.
- The σ_j are the uncertainties for every data point.

THE BAYESIAN SETUP

By updating a prior belief (i.e., a prior distribution) with given information (i.e., observed or fit data) and optimizing a likelihood function, a posterior distribution can be obtained according to Bayes' theorem.

- The prior
- The fit data
- The Log-Likelihood
- The sampling algorithm

The prior

The uniform prior

The prior preparation:

- The model parameters: g_σ, g_ω, g_ϱ, b, c, ξ, and Λ_ω
- Latin hypercube sampling (Loh, W.-L. 1996, AnSta, 24, 2058).
- Which provides relatively wide nuclear matter saturation properties.

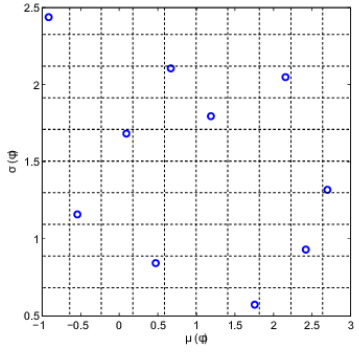

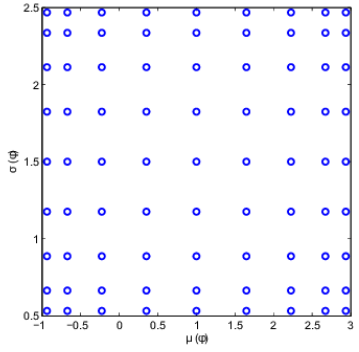

No	Parameters	*Set 0*	
		min	max
1	g_σ	6.5	15.5
2	g_ω	6.5	15.5
3	g_ϱ	6.5	15.5
4	B	0.5	9.0
5	C	-4.0	4.0
6	ξ	0.0	0.04 *
7	Λ_ω	0	0.12

*Note: We have also performed three identical studies but for three different ranges of a uniform prior for parameter ξ: i) $\xi = \in [0, 0.004]$ (*Set 1*), ii) $\xi \in [0.004, 0.015]$(*Set 2*) and iii) $\xi \in [0.015, 0.04]$ (*Set 3*).

The fit data

Constraints			
Quantity		Value/Band	Ref
NMP (MeV)	ρ_0	0.153 ± 0.005	Typel & Wolter (1999)
	ϵ_0	-16.1 ± 0.2	Dutra et al. (2014)
	K_0	230 ± 40	Todd-Rutel & Piekarewicz (2005); Shlomo et al. (2006)
	$J_{\mathrm{sym},0}$	32.5 ± 1.8	Essick et al. (2021a)
PNM (MeV fm^{-3})	$P(\rho)$	$2 \times \mathrm{N^3LO}$	Hebeler et al. (2013)
NS mass ($M_\odot$)	M_{max}	>2.0	Fonseca et al. (2021)

The Log-Likelihood

The equation 1 shows the log-likelihood function, except for the low-density PNM data and the maximum mass of NS. Our approach has been to use the box function probability as given in equation 2 for the PNM data from χEFT. We also used the step function probability for the NS mass.

$$Log(\mathcal{L}) = -0.5 \times \sum_j \left\{ \left(\frac{d_j - m_j(\theta)}{\sigma_j} \right)^2 + Log(2\pi\sigma_j^2) \right\} \quad (1)$$

$$Log(\mathcal{L}) = Log \left\{ \prod_j \frac{1}{2\sigma_j} \frac{1}{\exp\left(\frac{|d_j - m_j(\theta)| - \sigma_j}{0.015} \right) + 1} \right\} \quad (2)$$

†

[†] It is important to understand that when sampling the posterior, the normalization of the log-likelihood, which is done in equations 1 and 2 is irrelevant. However, to calculate the Bayes *evidence* it is mandatory and in some cases, it also reduces the computation time.

Sampling

Monte Carlo sampling:

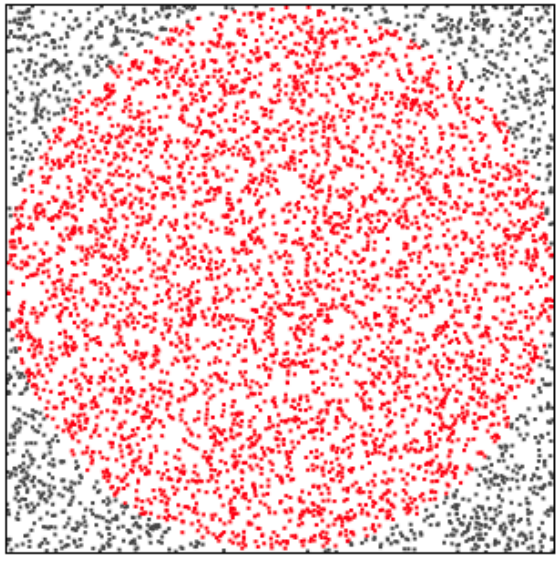

- Generate random uniform samples in the parameter hyperspace.
- Apply filter
- Analyze filtered samples' properties

Markov Chain Monte Carlo sampling:

- Cost-function guided random walk
- Sample the posterior

we use the nested sampling algorithm, first proposed in J Skilling, American Institute of Physics Conference Series, Vol. 735, edited by R. Fischer, R. Preuss, and U. V. Toussaint (2004) pp. 395–405.

- suitable for low-dimensional problems
- approximately 17000 samples we have obtained in the posterior

Results

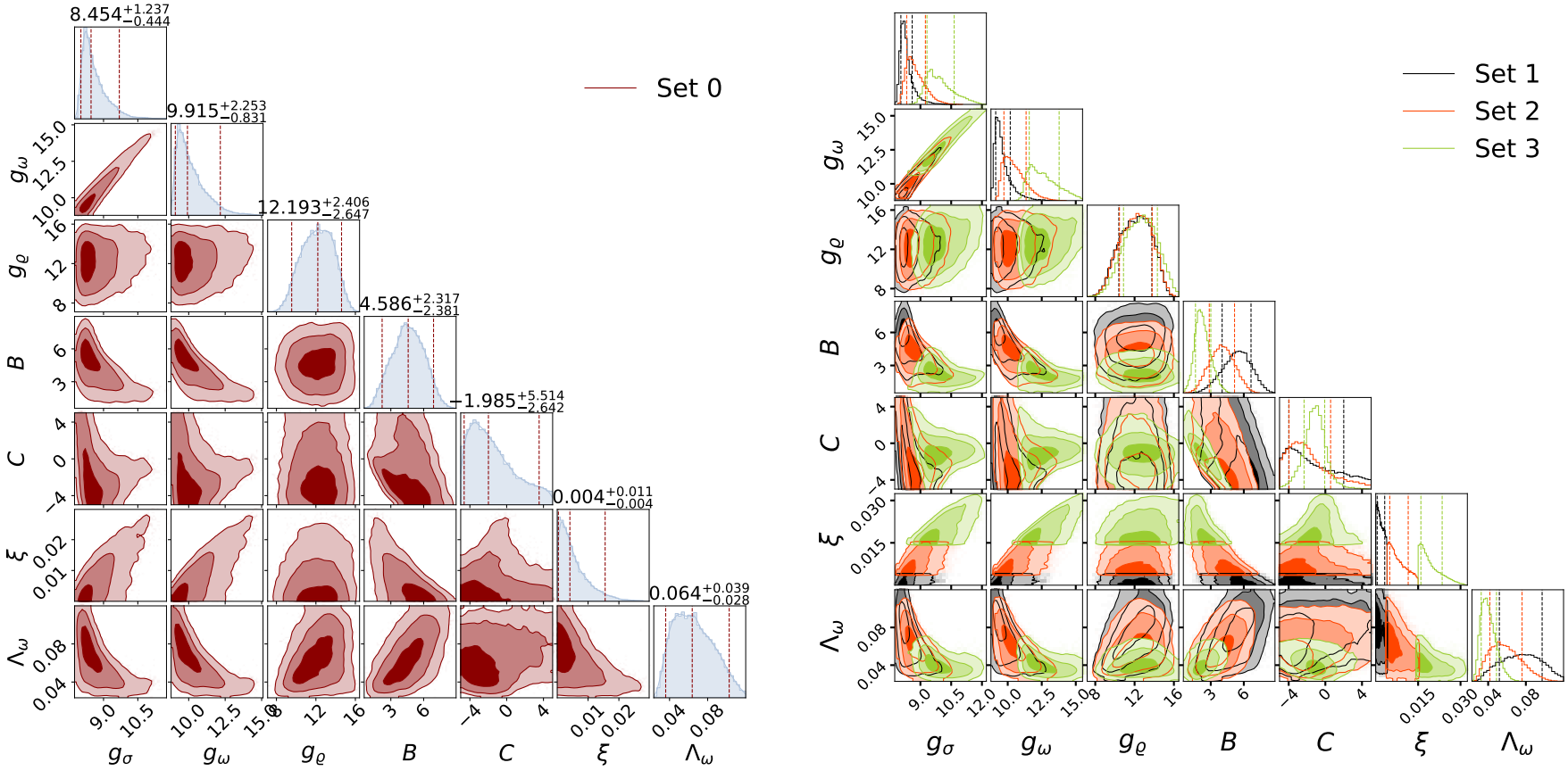

Corner plot for the three sets of models with Set 0 (dark red), Set 1 (black), Set 2 (orange), and Set 2 (green) comparing the posteriors of the parameters g_σ, g_ω, g_ρ, $B = b \times 10^3$, $C = c \times 10^3$, and Λ_ω of the RMF model used in present study. The vertical lines represent the 68% CIs, and the light and dark intensities represent the 1σ, 2σ, and 3σ CIs, respectively.

Results

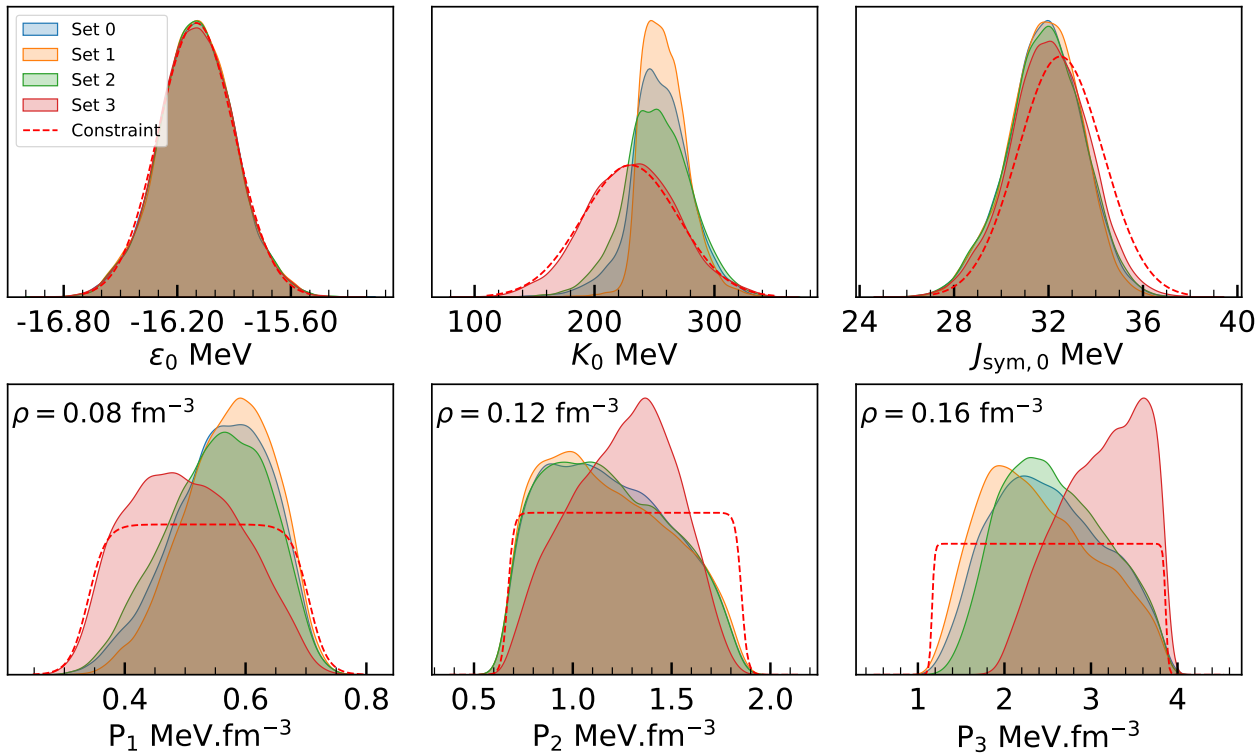

The comparison of the corresponding target distribution for the constraints imposed in the Bayesian inference analysis.

Nuclear matter properties

Posterior

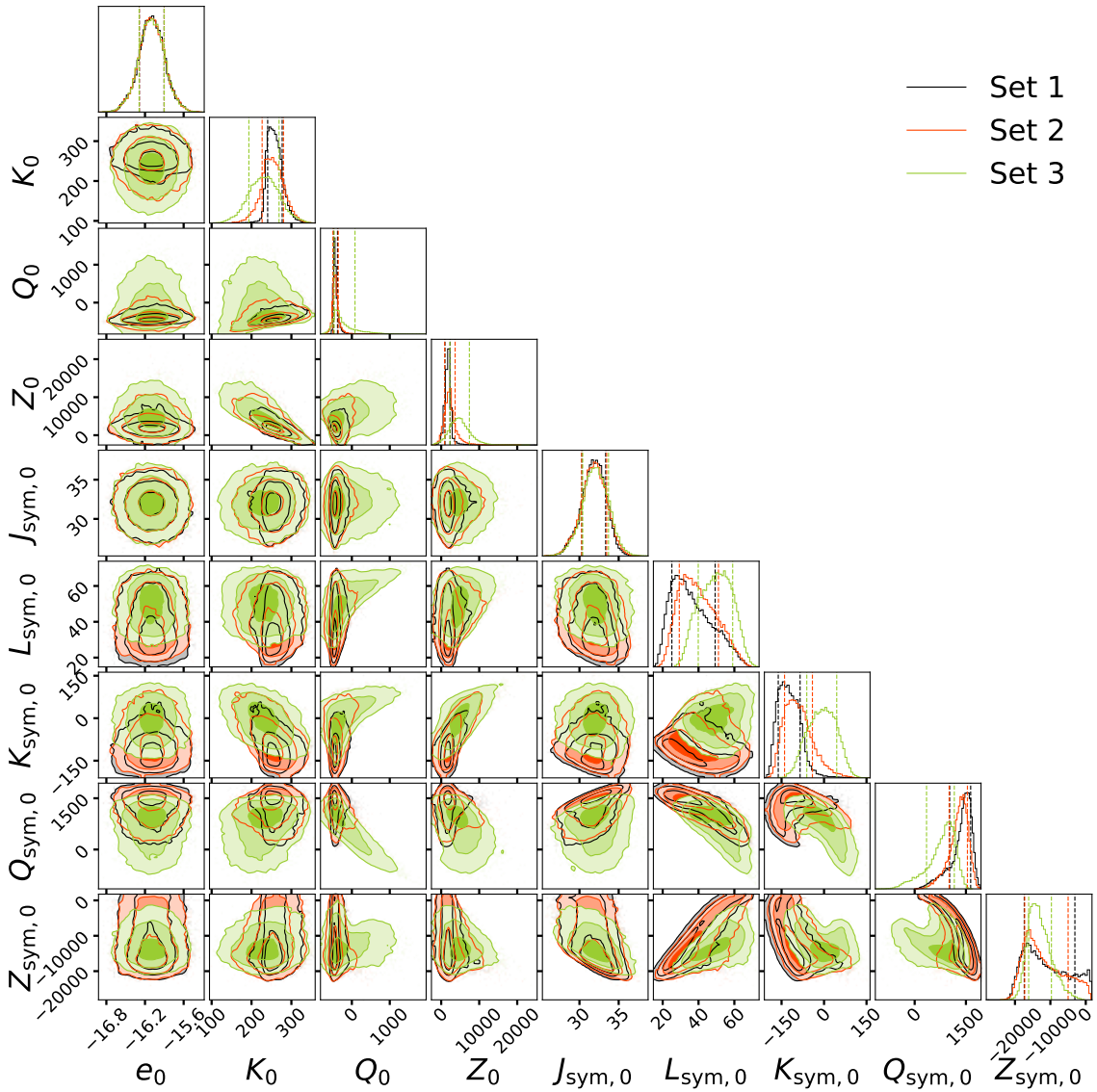

- Set 3 presents larger values of Q_0 and Z_0
- an anti-correlation between Z_0 and K_0: the lower values of K_0 are compensated by larger Z_0
- Set 3 also shows a slight positive correlation between $L_{\mathrm{sym},0}$ and $K_{\mathrm{sym},0}$, Similar behavior has been shown in Vidana et al, Phys.Rev.C 80 (2009) 045806.
- a strong correlation is obtained between $L_{\mathrm{sym},0}$ and $Q_{\mathrm{sym},0}$ for all three sets.

The NS properties

Posterior

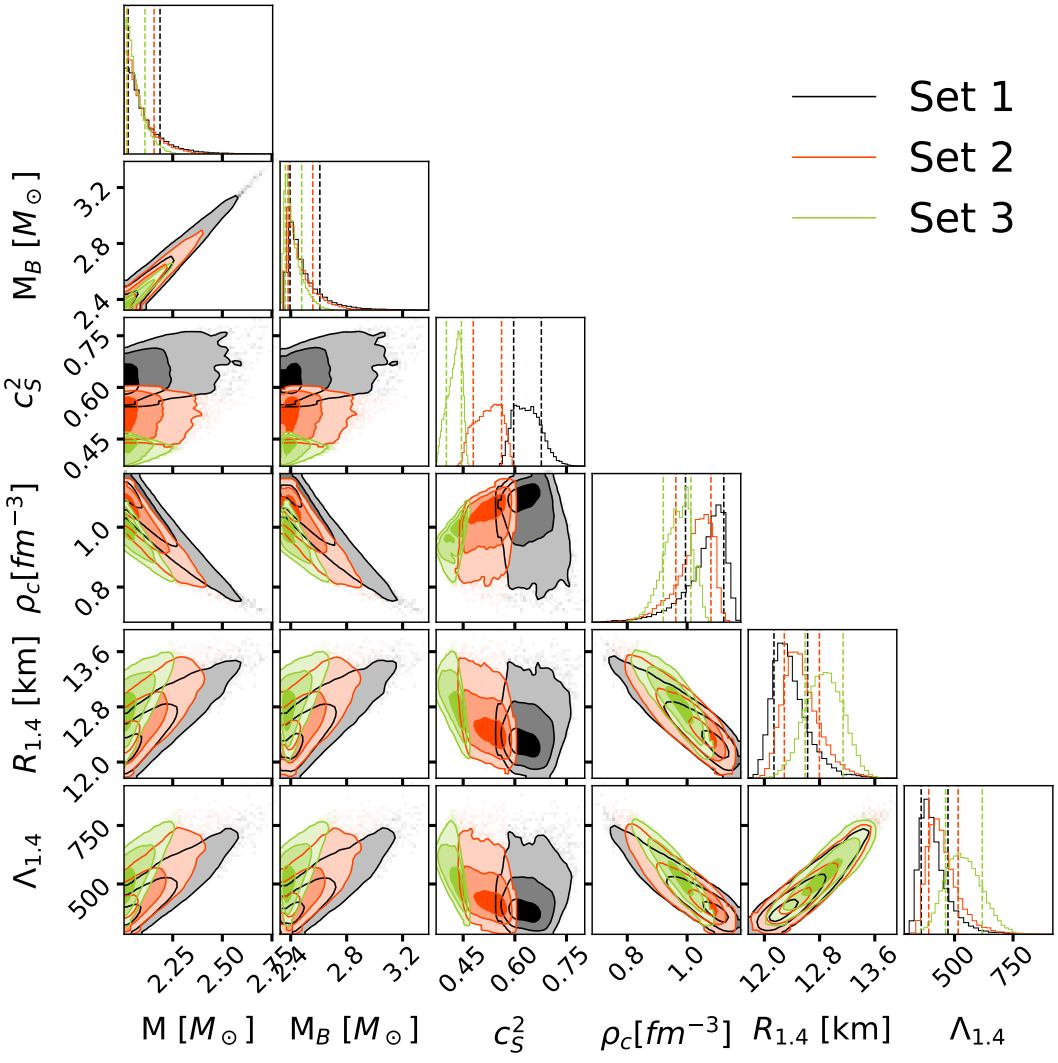

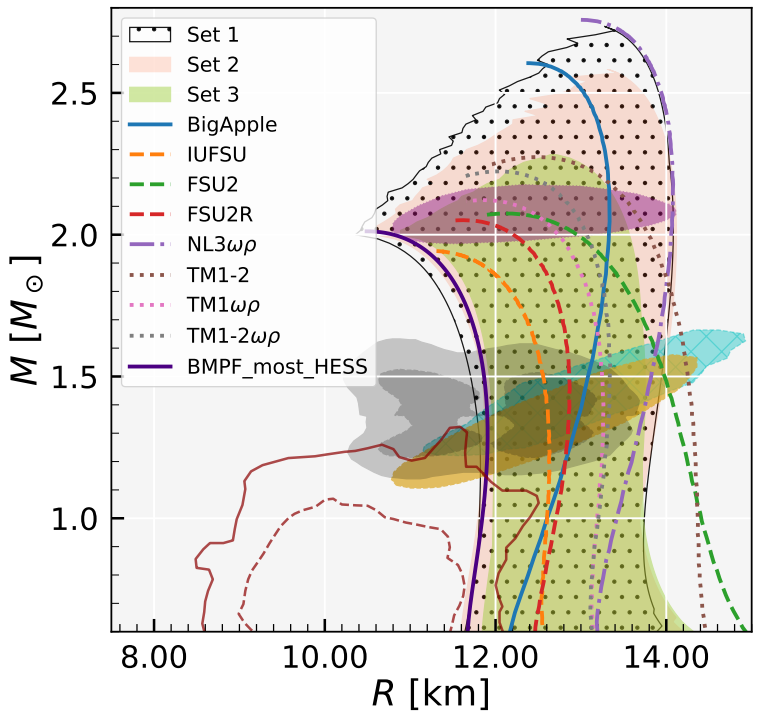

The NMP and NS properties

Quantity		Units	Set 1			Set 2			Set 3		
			median	90% CI min	90% CI max	median	90% CI min	90% CI max	median	90% CI min	90% CI max
NMP	ρ_0	fm^{-3}	0.152	0.145	0.160	0.152	0.145	0.160	0.153	0.145	0.161
	$m^\star$	...	0.76	0.69	0.78	0.72	0.64	0.76	0.63	0.55	0.69
	ε_0		−16.10	−16.43	−15.76	−16.10	−16.43	−15.76	−16.10	−16.43	−15.77
	K_0		257	234	293	252	205	300	232	169	295
	Q_0		−444	−497	−301	−438	−548	−256	−319	−562	483
	Z_0		1766	435	3054	2161	65	5521	4698	739	9623
	$J_{\mathrm{sym},0}$	MeV	31.87	29.10	34.22	31.90	29.05	34.44	32.05	29.19	34.75
	$L_{\mathrm{sym},0}$		35	21	57	39	25	58	50	35	64
	$K_{\mathrm{sym},0}$		−126	−177	−57	−96	−160	4	−6	−89	71
	$Q_{\mathrm{sym},0}$		1438	640	1736	1328	722	1661	866	−88	1303
	$Z_{\mathrm{sym},0}$		−12118	−19290	236	−13057	−19030	−1147	−13422	−17643	−6877
NS	M_{max}	$M_\odot$	2.073	2.013	2.306	2.064	2.011	2.244	2.048	2.010	2.162
	$M_{\mathrm{B},\mathrm{max}}$	$M_\odot$	2.457	2.378	2.772	2.437	2.367	2.677	2.400	2.348	2.546
	c_s^2	c^2	0.63	0.58	0.70	0.52	0.46	0.58	0.43	0.39	0.45
	ρ_c	fm^{-3}	1.079	0.914	1.138	1.036	0.899	1.099	0.972	0.883	1.035
	ε_c	$\mathrm{MeV\ fm}^{-3}$	1377	1169	1462	1302	1127	1394	1198	1084	1288
	R_{max}		10.75	10.46	11.52	11.03	10.69	11.74	11.47	11.07	11.97
	$R_{1.4}$		12.34	12.03	12.89	12.50	12.17	13.05	12.87	12.42	13.30
	$R_{1.6}$	km	12.21	11.89	12.86	12.39	12.04	13.02	12.77	12.31	13.26
	$R_{1.8}$		11.98	11.62	12.79	12.18	11.79	12.93	12.57	12.09	13.14
	$R_{2.075}$		11.67	10.96	12.86	11.88	11.21	12.92	12.25	11.65	12.96
	$\Lambda_{1.4}$		399	338	545	439	366	587	535	420	672
	$\Lambda_{1.6}$		156	129	233	174	141	250	215	166	284
	$\Lambda_{1.8}$	...	62	49	107	71	55	114	89	67	127
	$\Lambda_{2.075}$		17	9	42	20	12	43	26	16	43
	$\tilde{\Lambda}_{q=1.0}$		474	402	639	519	434	688	631	497	787

Conditional probabilities $P(R|M)$ and $P(\Lambda|M)$

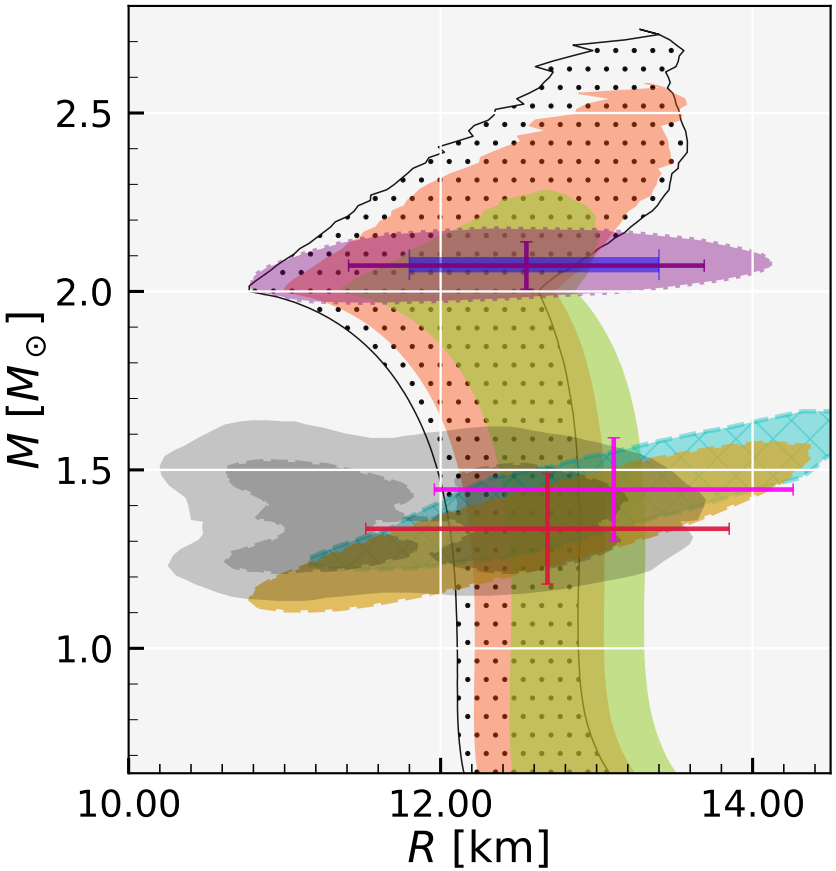

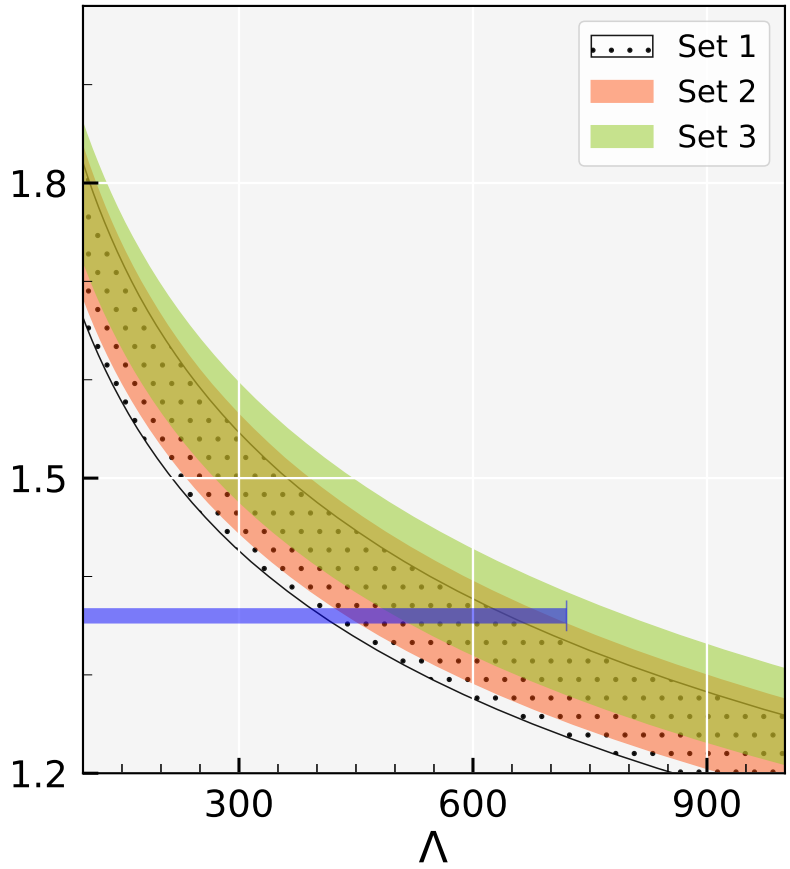

The Probability distribution of combined tidal deformability in BNS

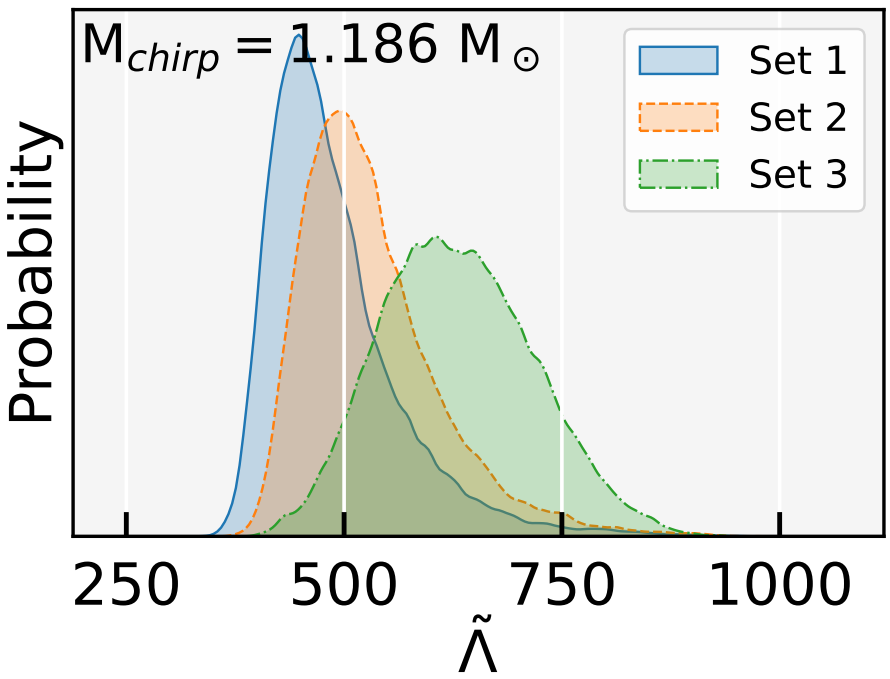

The $\tilde{\Lambda}$ in a Binary is plotted for a given *chirp* mass $M_{chirp} = 1.186\ M_\odot$.

- For each and every mass-radius curve, and fixing the chirp mass at $1.186 M_\odot$, we select all possible combinations of the mass m_1 and m_2 and calculate the combined tidal deformability. For each EOS we have 44 combinations of m_1 and m_2.
- The median and 90% CI for $\tilde{\Lambda}$ are:
  471^{+163}_{-71} (Set 1)
  516^{+166}_{-84} (Set 2)
  626^{+154}_{-132} (Set 3).

The proton fraction, symmetry energy and speed-of-sound

Posterior

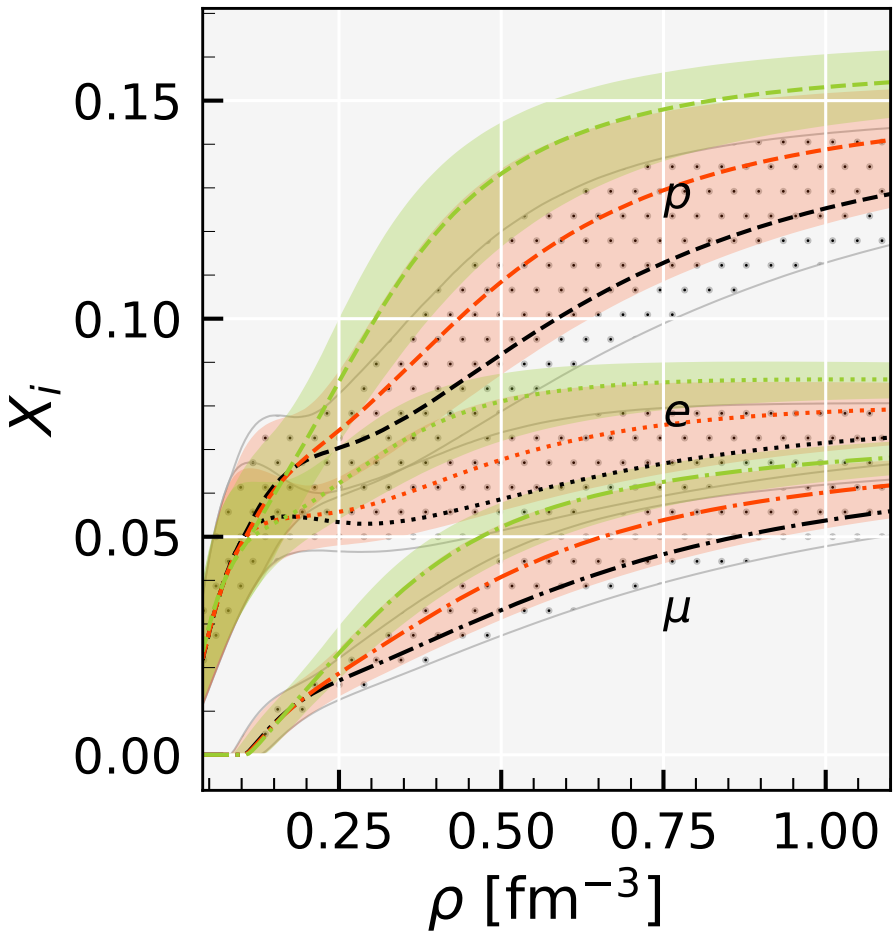

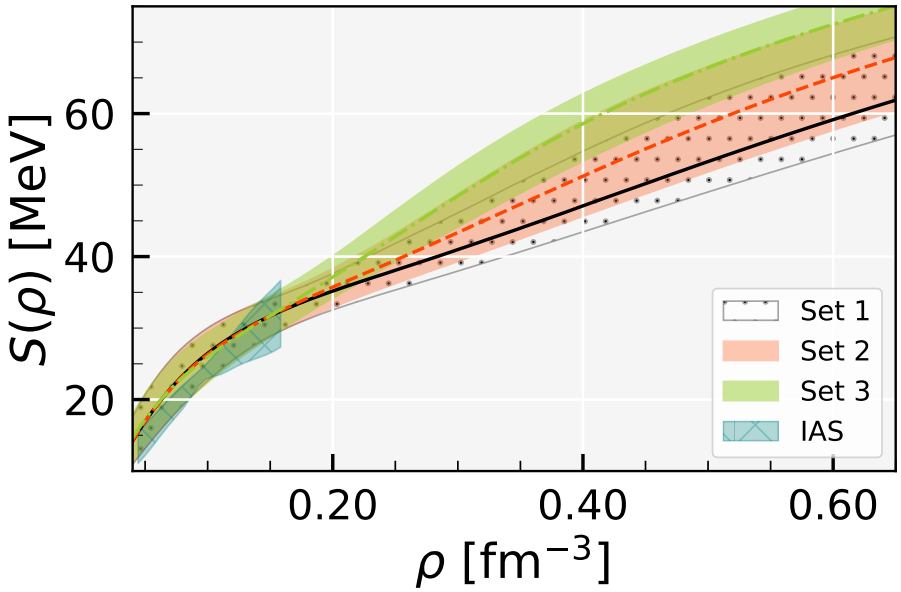

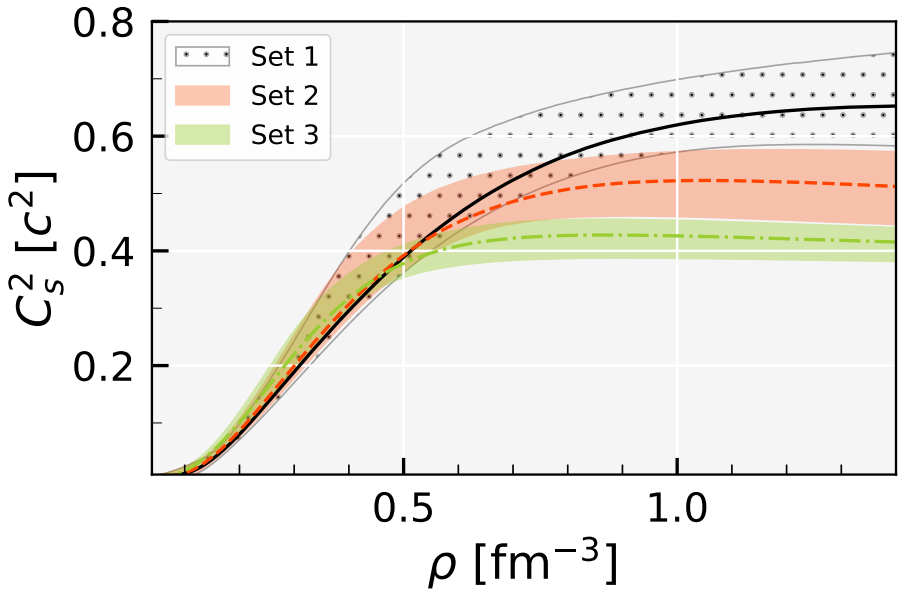

The correlation between the central density and its radius

The correlation coefficient between the central density of the maximum mass star ρ_c and its radius $R_{\rm max}$ is of the order of 0.9.

A similar result by J.-L. Jiang, C. Ecker, and L. Rezzolla, (2022), arXiv:2211.00018

$$\frac{\rho_c}{0.16\ \ \mathrm{fm}^{-3}} = d_0 \left[1 - \left(\frac{R_{\rm max}}{10\ \mathrm{km}}\right)\right] + d_1 \left(\frac{R_{\rm max}}{10\ \mathrm{km}}\right)^2 ,$$

with $d_0 = 27.6$ and $d_1 = 7.5$ and a 3.7% standard deviation of relative residual over the central value zero.

- Performing a similar analysis with Set 0, we have obtained $d_0 = 28.89 \pm 0.02$ and $d_1 = 7.73 \pm 0.01$.
- However, the linear relation shows a chi-square fit similar to the quadratic relation.

$$\frac{\rho_c}{0.16\ \ \mathrm{fm}^{-3}} = m_0 \left(\frac{R_{\rm max}}{10\ \mathrm{km}}\right) + c_0 ,$$

with $m_0 = -11.618 \pm 0.018$ and $c_0 = 19.255 \pm 0.019$.

Conclusion and future work

- The high-density behavior of nuclear matter is analyzed within a relativistic mean-field description with non-linear meson interactions
- Depending on the strength of the non-linear higher-order scalar vector field contribution, we have found three distinct classes of EOSs, each one correlated to different speed-of-sound density behavior.
- A weak non-linear vector contribution gives a monotonically increasing speed of sound
- The nuclear matter saturation properties (NMP) are very much model-dependent.
- Machine-Learning can be used to quantify the uncertainty of NMP due to different models and observations.

M Ferreira et al 2022 [arXiv:2209.09085]

ACKNOWLEDGMENTS

The authors acknowledge the Laboratory for Advanced Computing at the University of Coimbra for providing HPC resources (Navigator+) that have contributed to this research results.

Data availability

- arXiv:2301.08169 (2023)
- The final posterior of the model parameters, the equation of states, and the solutions for the star properties obtained with prior Set 0 can be obtained from the link **(http://e.pc.cd/moqotalK)**.

Thank you!

Obrigado!